

# Identification of key genes in diabetic nephropathy based on lipid metabolism

MENG YANG, JIAN WANG, HU MENG, JIAN XU, YU XIE and WEIYING KONG

Department of Nephrology, The First People's Hospital of Yunnan Province, The Affiliated Hospital of Kunming University of Science and Technology, Kunming, Yunnan 650032, P.R. China

Received December 2, 2023; Accepted June 20, 2024

DOI: 10.3892/etm.2024.12695

**Abstract.** Diabetic nephropathy (DN) is a common systemic microvascular complication of diabetes with a high incidence rate. Notably, the disturbance of lipid metabolism is associated with DN progression. The present study aimed to identify lipid metabolism-related hub genes associated with DN for improved diagnosis of DN. The gene expression profile data of DN and healthy samples (GSE142153) were obtained from the Gene Expression Omnibus database, and the lipid metabolism-related genes were obtained from the Molecular Signatures Database. Differentially expressed genes (DEGs) between DN and healthy samples were analyzed. The weighted gene co-expression network analysis (WGCNA) was performed to examine the relationship between genes and clinical traits to identify the key module genes associated with DN. Next, the Venn Diagram R package was used to identify the lipid metabolism-related genes associated with DN and their protein-protein interaction (PPI) network was constructed. Subsequently, Gene Ontology (GO) and Kyoto Encyclopedia of Genes and Genomes (KEGG) enrichment analyses were performed. The hub genes were identified using machine-learning algorithms. The Gene Set Enrichment Analysis (GSEA) was used to analyze the functions of the hub genes. The present study also investigated the immune infiltration discrepancies between DN and healthy samples, and assessed the correlation between the immune cells and hub genes. Finally, the expression levels of key genes were verified by reverse transcription-quantitative (RT-q)PCR. The present study determined 1,445 DEGs in DN samples. In addition, 694 DN-related genes in MEyellow and METurquoise modules were identified by WGCNA. Next, the Venn Diagram

R package was used to identify 17 lipid metabolism-related genes and to construct a PPI network. GO analysis revealed that these 17 genes were markedly associated with 'phospholipid biosynthetic process' and 'cholesterol biosynthetic process', while the KEGG analysis showed that they were enriched in 'glycerophospholipid metabolism' and 'fatty acid degradation'. In addition, SAMD8 and CYP51A1 were identified through the intersections of two machine-learning algorithms. The results of GSEA revealed that the 'mitochondrial matrix' and 'GTPase activity' were the markedly enriched GO terms in both SAMD8 and CYP51A1. Their KEGG pathways were mainly concentrated in the 'pathways of neurodegeneration-multiple diseases'. Immune infiltration analysis showed that nine types of immune cells had different expression levels in DN (diseased) and healthy samples. Notably, SAMD8 and CYP51A1 were both markedly associated with activated B cells and effector memory CD8 T cells. Finally, RT-qPCR confirmed the high expression of SAMD8 and CYP51A1 in DN. In conclusion, lipid metabolism-related genes SAMD8 and CYP51A1 may play key roles in DN. The present study provides fundamental information on lipid metabolism that may aid the diagnosis and treatment of DN.

## Introduction

The prevalence of diabetes mellitus is increasing annually worldwide; it is estimated that by 2030, the global diabetic population will reach approximately 4.39 billion (1). Diabetic nephropathy (DN), one of the most common and serious systemic microvascular complications of diabetes (2). A previous study reported a prevalence rate of DN among Chinese adults as high as 30.9% in the diabetic population and identified DN as a major cause of end-stage renal disease (ESRD) worldwide (3). Therefore, it is essential to implement proactive and early preventative and treatment strategies for delaying the progression of DN to ESRD (4-6). The incidence of DN is generally considered to vary based on genetic background and some associated risk factors (7), and DN is considered to result from the interaction between hemodynamic and metabolic factors. Its pathogenesis involves multiple factors and pathways, including lipid metabolism disorders and renal ectopic lipid accumulation (8-10).

DN is mainly characterized by glomerular damage and tubulointerstitial lesions. It has a complex pathogenesis,

---

*Correspondence to:* Dr Meng Yang, Department of Nephrology, The First People's Hospital of Yunnan Province, The Affiliated Hospital of Kunming University of Science and Technology, 157 Jinbi Road, Kunming, Yunnan 650032, P.R. China  
E-mail: 13648897447@126.com

**Key words:** diabetic nephropathy, weighted gene co-expression network analysis, lipid metabolism-related hub genes, immune infiltration

involving nephritis, interstitial fibrosis (also known as pulmonary fibrosis), renal tubular atrophy and abnormal lipid metabolism (11-14). There is growing evidence that dyslipidemia plays a crucial role in the development of DN (11,15). Patients with DN often present with significant dyslipidemia. In dyslipidemia, high level of triglycerides, low levels of HDL cholesterol and lipoproteins with altered composition are transported and deposited in the kidney. This process activates the inflammatory responses and causes oxidative stress, mitochondrial dysfunction and cell death, thereby damaging the kidney (12,16-19). A previous study has shown that changes in renal triglyceride and cholesterol metabolism can lead to lipid accumulation in DN, and there is a highly significant association between renal function, inflammation and lipid metabolism-related genes (11). Another study explored the role of annexin A1 (ANXA1) in diabetic mice and proximal tubular epithelial cells (PTECs) treated with high glucose plus palmitic acid and found that ANXA1 may regulate lipid metabolism in PTECs, thereby improving disease progression (20). Disordered lipid metabolism is a key factor responsible for DN progression. Ectopic lipid deposition is aggravated in DN, which promotes tubular cell inflammation and apoptosis. As a result, DN-induced pathological changes are further aggravated (21-23). Diacylglycerol, triacylglycerol (TAG), and lysophosphatidylcholine (LPC) are significantly upregulated in patients with DN (19). Among these, phosphatidylethanolamine (PE) is an important multifunctional glycerophospholipid, and its metabolic abnormalities are closely associated with lipid metabolism disorders in DN (24-27), but the regulatory role of lipid metabolism-related genes in DN remains to be elucidated.

Bioinformatics methods are powerful tools for identifying potential key genes involved in a disease. Therefore, they have attracted increasing attention in recent years for analyzing microarray data. The present study investigated the influence of lipid metabolism on DN by analyzing lipid metabolism-related genes through machine-learning algorithms and integrating their potential functional pathways. In addition, it performed immune infiltration analysis to explore the association between key genes of lipid metabolism and immune cells. Finally, it verified these key genes by reverse transcription-quantitative (RT-q)PCR.

## Materials and methods

**Data source.** Gene expression profiles from the GSE142153 dataset (28), comprising data from peripheral blood samples obtained from 23 patients with DN and 10 healthy controls, were downloaded from the Gene Expression Omnibus database ([ncbi.nlm.nih.gov/geo/](https://ncbi.nlm.nih.gov/geo/)), which was obtained from the GPL6480 platform (Table SI). This dataset included microarray data, which were presented in the form of raw signal intensities or gene expression levels. In addition, 904 lipid metabolism-related genes were acquired from the Molecular Signature Database (<https://www.gsea-msigdb.org/gsea/msigdb>).

**Differential expression analysis.** The present study employed the R package limma (29) to analyze the differentially expressed genes (DEGs) between DN and healthy samples in

the GSE142153 dataset, based on the criteria  $\log_2FCI > 0.5$  and  $P < 0.05$ . Next, the ggplot2 (30) and pheatmap (31) packages in R (version 4.0.2, 2020, R-project.org/) were used to generate the volcano plot and heatmap of DEGs, respectively.

**Weighted gene co-expression network analysis (WGCNA).** To find the genes linked with DN, the WGCNA package in R (32) was performed to construct a co-expression network based on the 23 DN samples and 10 healthy samples in the GSE142153 dataset. First, to ensure the accuracy of the analysis, these samples were clustered to remove the outliers. Next, to ensure the interactions of genes accord with the scale-free distribution to the maximum extent, the soft threshold of all data was determined. Subsequently, the dissimilarity coefficients of genes were calculated and the systematic clustering tree was obtained. For each gene module, the minimum module size was set as 150 with the criteria of the dynamic tree cutting, and similar modules were merged. Ultimately, the relationships among the modules and clinical traits (DN and healthy) were calculated to identify the key modules (correlation coefficient  $|cor| \geq 0.6$ ,  $P \leq 0.05$ ). Module membership (MM) correlation between key module genes and the modules, and the gene significance (GS) correlation between key module genes and clinical traits were further calculated to identify the genes in DN ( $IMMI > 0.8$  and  $IGSI > 0.2$ ) (33).

**Identification and protein-protein interaction (PPI) of the lipid metabolism-related genes in DN.** The present study intersected DEGs, key module genes and 904 lipid metabolism-related genes to identify lipid metabolism-related genes in DN using the Venn Diagram R package (34). The associations among these genes were determined. In addition, a PPI network was constructed using STRING (<https://cn.string-db.org/>) database (confidence=0.15) (35) to analyze the interaction between the proteins of lipid metabolism-related genes in DN.

**Functional enrichment analysis.** Gene Ontology (GO) and Kyoto Encyclopedia of Genes and Genomes (KEGG) analyses were performed to investigate the potential role of lipid metabolism-related genes in DN using the clusterProfiler R package (36). The results were visualized using GOplot (37) and the enrichplot package (38).

**Screening and Gene Set Enrichment Analysis (GSEA) of lipid metabolism-related hub genes in DN.** To identify the hub genes of lipid metabolism in DN, two classification models were established using 23 DN and 10 healthy samples: The Least Absolute Shrinkage and Selector Operation (LASSO) algorithm model in R package glmnet (39) and the Support Vector Machine-Recursive Feature Elimination (SVM-RFE) algorithm model in R package e1071 (40). The efficiency of these two models was determined using a 10-fold cross-validation method. The intersections of the results obtained using these two models were employed as the lipid metabolism-related hub genes in DN for the subsequent research. In addition, the R package clusterProfiler (36) was used to perform GSEA of the hub genes. The correlations between hub genes and other genes was determined using the default gene sets in the org.Hs.eg.db package (version 3.12.0, [bioconductor.org/packages/release/data/annotation/html/org.Hs.eg.db.html](https://bioconductor.org/packages/release/data/annotation/html/org.Hs.eg.db.html)). The

significance thresholds were  $|\text{Normalized Enrichment Score (NES)}| > 1$ ,  $P < 0.05$  and  $q < 0.2$ .

**Immune infiltration evaluation.** To investigate discrepancies in immune cell infiltration between the DN and healthy samples, the present study evaluated 28 types of immune cell infiltrations in the 23 DN and 10 healthy samples in the GSE142153 dataset using the ‘ssGSEA’ method in the GSVA R package (41). A heatmap was plotted of the ssGSEA scores of immune cells for each sample. The various immune cells between DN and healthy samples were evaluated using Wilcoxon rank-sum test and the results were visualized through the Vioplot package (version 0.3.7; github.com/TomKellyGenetics/vioplot). Ultimately, the Pearson correlation coefficients between each immune cell, the immune cells and hub genes were calculated and visualized using corrplot package in R (42).

**RT-qPCR.** The present study collected peripheral blood mononuclear cell samples from 10 healthy subjects and 10 patients with DN from the First People's Hospital of Yunnan Province (Kunming, China). The patient samples were collected between 1 and 30 March, 2022. All subjects provided written informed consent before participating in the study. The present study was approved by the Ethics Committee of The First People's Hospital of Yunnan Province (approval no. 2022GJ227).

First, RNA was extracted using TRIzol® (Invitrogen; Thermo Fisher Scientific, Inc.). RT was performed with SweScript First-Strand cDNA Synthesis Kit (Servicebio, Wuhan, China) according to the manufacturer's protocols. qPCR was performed strictly according to the manufacturer's instructions for 2xUniversal Blue SYBR Green qPCR Master Mix (Servicebio, Wuhan, China). qPCR reaction mixture comprised 3  $\mu\text{l}$  of cDNA, 5  $\mu\text{l}$  of 2xUniversal Blue SYBR Green qPCR Master Mix (Servicebio, Wuhan, China) and 1  $\mu\text{l}$  of forward and reverse primer (Tsingke, China) also at a concentration of 10  $\mu\text{M}$ . qPCR was performed using the CFX96 Real-Time PCR Detection System (Bio-Rad, China) according to the following steps: pre-denaturation at 95°C for 1 min, followed by 40 cycles of denaturation at 95°C for 20 sec, annealing at 55°C for 20 sec, and extension at 72°C for 30 sec. GAPDH was used as the internal reference gene, and the relative expression levels of key genes were calculated using the  $2^{-\Delta\Delta C_q}$  method (43). All systematic analyses were performed in triplicate. qPCR primer sequences are shown in Table I.

**Statistical analysis.** All analyses were carried out in R language (version 4.0.2). Differences between groups were analyzed by Wilcoxon rank-sum test.  $P < 0.05$ . The Independent-samples t-test was employed. Assuming normal distribution and equal variances, the mean and SEM) were calculated for each group. All systematic analyses were performed in triplicate.

## Results

**Identification of DEGs.** The present study identified 1,445 DEGs between the DN and healthy samples in the GSE142153 dataset. Among the DEGs present in DN samples, 707 genes

Table I. Reverse transcription-quantitative PCR primer sequences.

Primer	Sequence, 5'-3')
SAMD8	F: CCTTTCATCAGTGCTCTTCAGA R: AATCATGCCACATACTTCCGTC
CYP51A1	F: TAAGGCAATCCAGAAACGCA R: CCAAAAAGAAGCCCATCCAA
$\beta$ -actin	F: GGAAGGTGAAGGTCGGAGT R: TGAGGTCAATGAAGGGGTC

F, forward; R, reverse.

were upregulated and 738 were downregulated. A volcano plot and a heatmap of these genes are in Fig. 1.

**Screening of genes in key modules by WGCNA.** A sample clustering tree after excluding the outliers (GSM4221586) was plotted (Fig. 2A and B). The network accorded with the scale-free distribution to the maximum extent possible when the soft threshold was 7 (Fig. 2C). After determining the soft threshold, the gene dendrogram was constructed and 15 co-expression modules were found by setting the minimum module size at 150 (Fig. 2D). The correlations among the modules and DN and healthy samples showed that MEyellow was positively correlated with DN, whereas METurquoise had a negative correlation with DN (Fig. 2E). Finally, 694 DN-related genes in MEyellow and METurquoise with  $|\text{MMI}| > 0.8$  and  $|\text{GSI}| > 0.2$  were identified (Fig. 2F and G).

**Identification and PPI of the lipid metabolism-related genes in DN.** A Venn diagram was used to identify 17 genes associated with lipid metabolism in DN through the intersections of 1,445 DEGs, 694 DN-related genes in the MEyellow and METurquoise modules, and 904 lipid metabolism-related genes (Fig. 3A). The correlation analysis among these 17 genes demonstrated a strong correlation between IDI1 and PTS (Fig. 3B). The aforementioned 17 lipid metabolism-related genes were then uploaded into the STRING database. However, the SAMD8 and TNFAIP8L2 genes were excluded from the STRING database as they did not show any interaction. Next, a PPI network of 15 genes with a confidence of 0.15 was constructed. The degree scores of these 15 genes are shown in a bar chart (Fig. 3C and D).

**Functional enrichment analyses.** GO and KEGG functional enrichment analyses were conducted to investigate the potential functions of the 17 lipid metabolism-related genes implicated in DN. Notably, 5 KEGG pathways and 23 GO entries belonging to the biological process (BP) category were identified ( $P_{\text{adjust}} < 0.05$  and count  $> 2$ ). The BP results showed that these 17 lipid metabolism-related genes were closely associated with the ‘phospholipid biosynthetic process’, ‘alcohol biosynthetic process’ and ‘cholesterol biosynthetic process’ (Fig. 4A). The KEGG analysis demonstrated that the markedly enriched pathways associated with these genes included ‘glycerophospholipid metabolism’, ‘steroid biosynthesis’ and ‘fatty acid degradation’ (Fig. 4B).

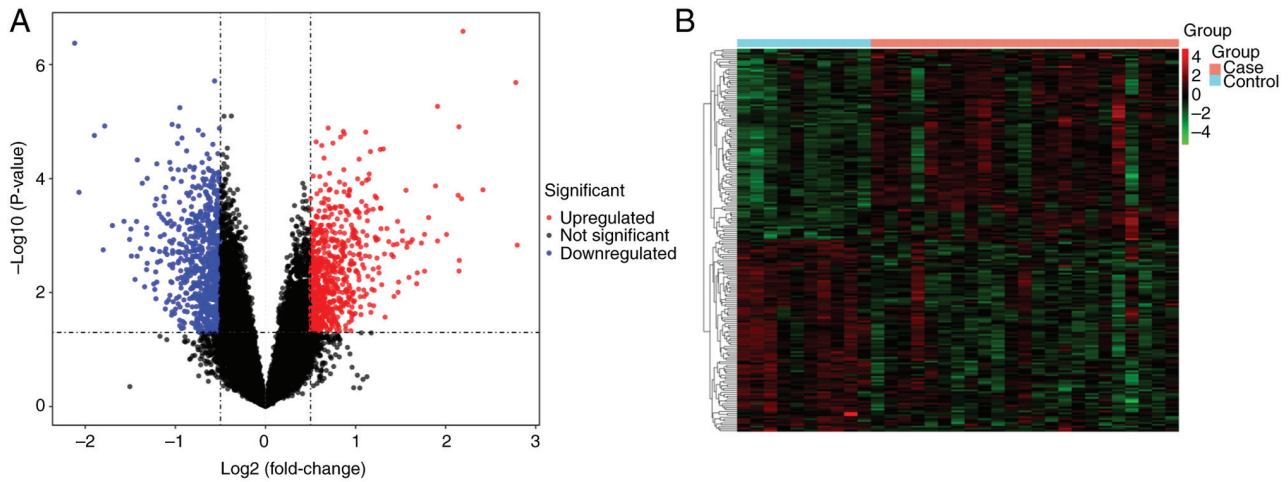


Figure 1. Analysis of differentially expressed genes. (A) Volcano plot of differences between DN and healthy groups. Red dots indicate that the gene expression is upregulated (DN vs. healthy samples), blue dots indicate that the gene expression is downregulated, and black dots indicate the difference is not significant. (B) Heatmap plot of differences between DN and healthy groups. Blue represents DN samples and red represents control samples. The higher the expression, the darker the color. DN, diabetic nephropathy.

**Identification and GSEA of hub genes.** To identify hub genes among the aforementioned 17 lipid metabolism-related genes, LASSO and SVM-RFE algorithm models were established based on the data obtained from 23 DN samples and 10 healthy samples. LASSO algorithm identified four genes as feature genes (Fig. 5A and B). Three genes were identified as feature genes by the SVM-RFE algorithm (Fig. 5C), which are the first three genes in Table SII. The intersections of these two algorithm models revealed two overlapping genes, *SAMD8* and *CYP51A1* (Fig. 5D). The top 10 most important GO and KEGG terms of the GSEA results of *SAMD8* and *CYP51A1* were screened. ‘mitochondrial matrix’ and ‘GTPase activity’ were identified as the common markedly enriched GO term in both *SAMD8* and *CYP51A1* (Fig. 5E and G). The following common markedly enriched KEGG pathways for *SAMD8* and *CYP51A1* were identified: ‘Alzheimer disease’, ‘IL-17 signaling pathway’, ‘pathways of neurodegeneration-multiple diseases’ and ‘TGF-beta signaling pathway’ (Fig. 5F and H).

**Immune infiltration analysis.** The ssGSEA was employed to evaluate the infiltration levels of 28 immune cell types in both DN and healthy samples. A heatmap displaying the ssGSEA scores is shown in Fig. 6A. A total of nine immune cell types were significantly different between DN and healthy samples: Activated B cells, CD56bright natural killer cells, effector memory CD4 T cells, effector memory CD8 T cells, mast cells, memory B cells, plasmacytoid dendritic cells, T follicular helper cells and type 1 T helper cells. These cell types exhibited significant differences between the DN and healthy samples, as visualized using a violin chart (Fig. 6B). Furthermore, the Pearson correlation coefficients of the immune cell types showed that monocytes exhibited a markedly positive correlation with plasmacytoid and immature dendritic cells (Fig. 6C). Finally, the Pearson correlation coefficients between immune cells and hub genes (*SAMD8* and *CYP51A1*) were calculated. *SAMD8* and *CYP51A1* were both correlated with the activated B cells, effector memory CD8 T

cells, memory B cells and T follicular helper cells ( $|cor| > 0.4$ ; Fig. 6D and E).

**Expression of *SAMD8* and *CYP51A1*.** The RT-qPCR analysis showed a higher expression of *SAMD8* and *CYP51A1* in DN samples than in those from normal subjects, which was consistent with the aforementioned results of the present study (Fig. 7A and B).

## Discussion

Lipid metabolism plays an important role in the progression of DN, but the specific mechanism of action between the two remains to be elucidated. The present study identified two hub genes, *SAMD8* and *CYP51A1*, using LASSO and SVM-RFE algorithms. *SAMD8*, which encodes sphingomyelin synthase-related protein (SMSr), is located in the cytosol and endoplasmic reticulum, and acts as a component of the endoplasmic reticulum membrane (44). *SAMD8* can participate in the regulation of ceramide biosynthesis by activating ceramide choline phosphotransferase and sphingomyelin synthase activities. Tafesse *et al* (45) reported that *SAMD8* acts as a suppressor of ceramide-mediated apoptosis. Notably, disruption of the catalytic activity of SMSr can increase the endoplasmic reticulum ceramide levels and mislocalize them to the mitochondria, triggering the mitochondrial apoptosis pathway (45). The association between ceramide and DN has been reported (46). Notably, ceramides are abundant in the kidney, and they regulate diverse cellular events, including differentiation, growth arrest and apoptosis (47-49). Studies on humans and animal models have demonstrated that the accumulation of lipids and their metabolites in tissues, including those of the kidney, can cause lipid toxicity (50,51). Reducing the accumulation of ceramide may improve insulin resistance, steatohepatitis and other metabolic disorders (52). Therefore, it was hypothesized that *SAMD8* could be implicated in DN by affecting the synthesis of ceramide.

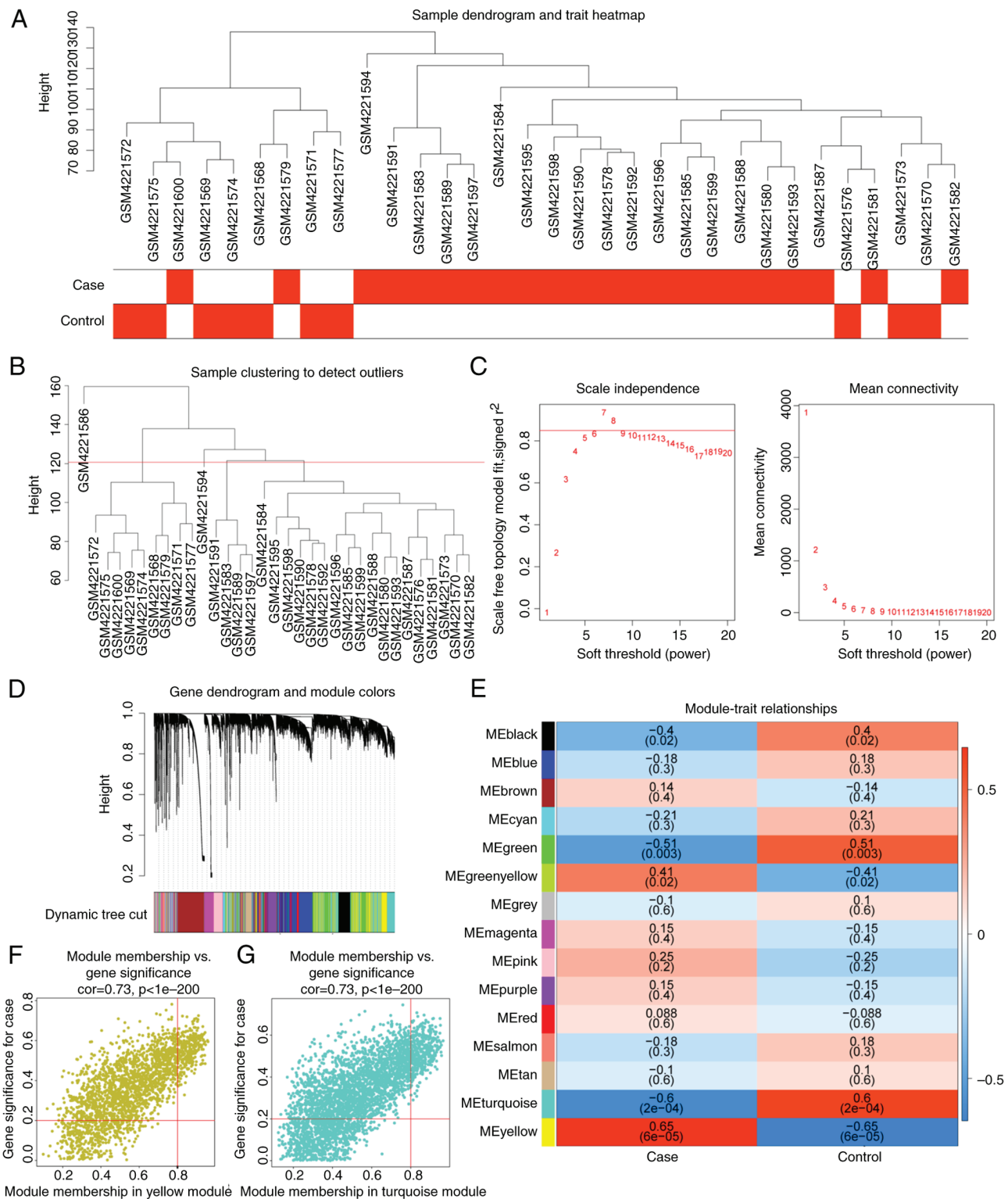


Figure 2. WGCNA. (A) Sample dendrogram and trait heatmap. The clustering was based on the expression data of DN samples. The genes with the highest average expression values were used for WGCNA. The red color was proportional to DN trait. (B) Cluster analysis of DN samples. The red line was used to distinguish the outlier samples. The threshold was set as 140 and one outlier sample, that is, GSM4221586, was identified. (C) Soft threshold filtering. Analysis of the scale-free fit index for various soft-thresholding powers ( $\beta$ ). In all, 7 was the greatest fit power value. (D) Gene dendrogram and module colors. The cluster dendrogram of co-expression genes in DN. Each branch in the figure represents one gene and every color below represents one co-expression module. (E) Heatmap of association between module eigengenes and DN. The turquoise and yellow modules were the most associated with DN. (F) Module membership in yellow module was the most positively correlated with DN. (G) Module membership in turquoise module was the most negatively correlated with DN. DN, diabetic nephropathy; WGCNA, weighted gene co-expression network analysis.

CYP51A1, a member of the cytochrome P450 superfamily of enzymes, catalyzes the removal of the 14-methyl group in

lanosterol, a key step in the synthesis of cholesterol (53,54). Patients with DN are characterized by an increased plasma

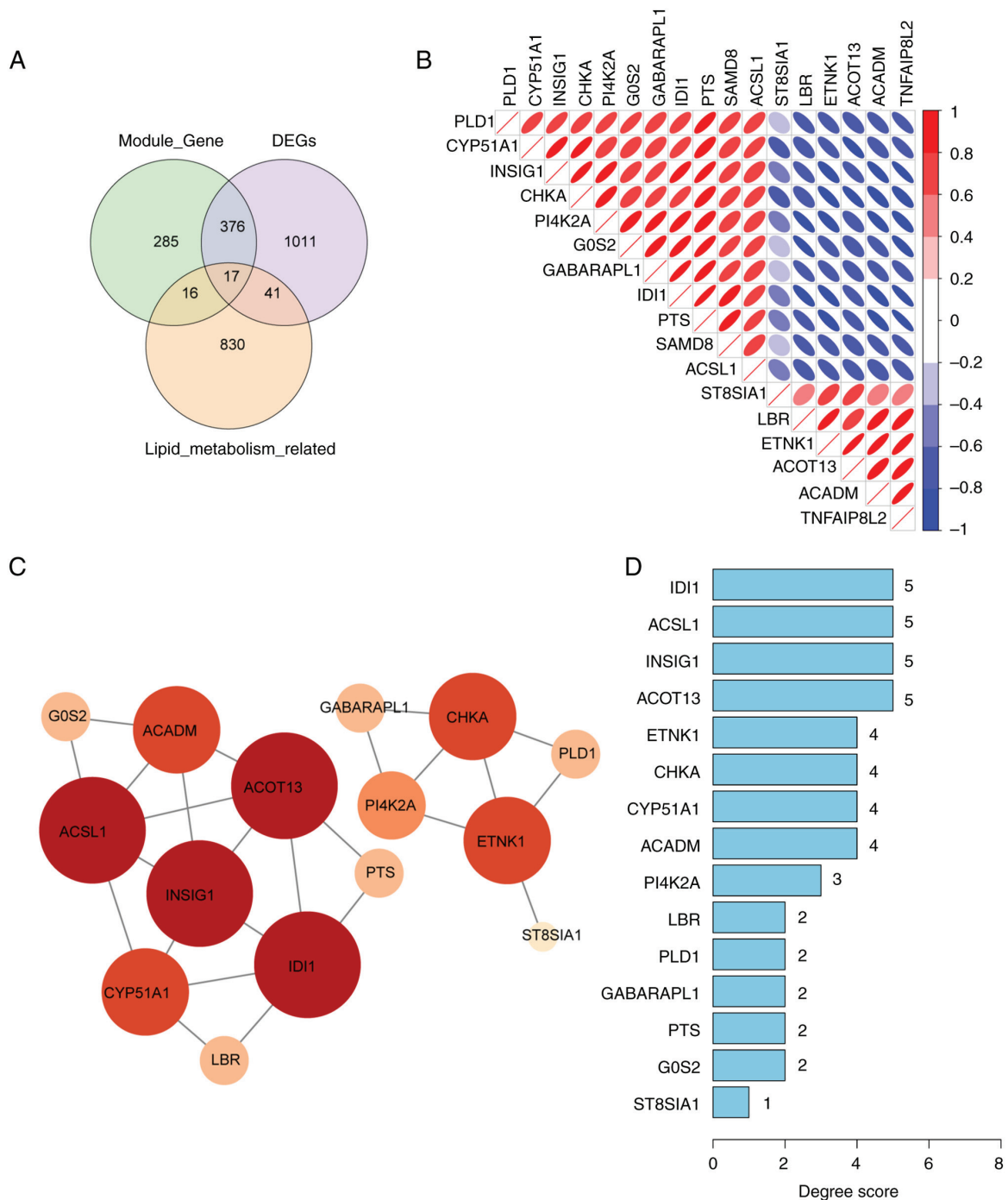


Figure 3. PPI network of hub genes. (A) A Venn diagram revealed 17 key genes among lipid metabolism-related genes, Module Gene and DEGs by overlapping them. (B) Expression correlation analysis revealed IDI1 and PTS had a notable correlation among these 17 genes. (C) PPI network of 15 genes, removing SAMD8 and TNFAIP8L2. Edges indicate interaction between two genes. Degree indicates the number of edges directly connected to a node. A node with a higher Degree has more connections in the network and thus exerts greater influence. (D) Degree scores of the PPI network. DEGs, differentially expressed genes; PPI, protein-protein network.

concentration of cholesterol (15), reduced expression of lipoprotein lipase, disruption of reverse cholesterol transport and reduced number of receptors mediating lipid uptake (8). Therefore, CYP51A1 could be involved in the development of DN by regulating cholesterol synthesis. However, to the best of our knowledge, the role of SAMD8 and CYP51A1 in DN has not been reported, and the present study was the first to discover the role of two key genes in DN, which may provide a new target for the treatment of DN.

The KEGG analysis of the 17 lipid metabolism-related genes identified the following representative pathways: ‘Glycerophospholipid metabolism’, ‘steroid biosynthesis’ and ‘fatty acid degradation’. Notably, all the terms (‘phospholipid biosynthetic process’, ‘alcohol biosynthetic process’, and ‘cholesterol biosynthetic process’) identified through GO analysis are from the BP category. Studies have shown that abdominal subcutaneous fat deposition and elevated non-esterified fatty acids (NEFA) in plasma, which are characteristics

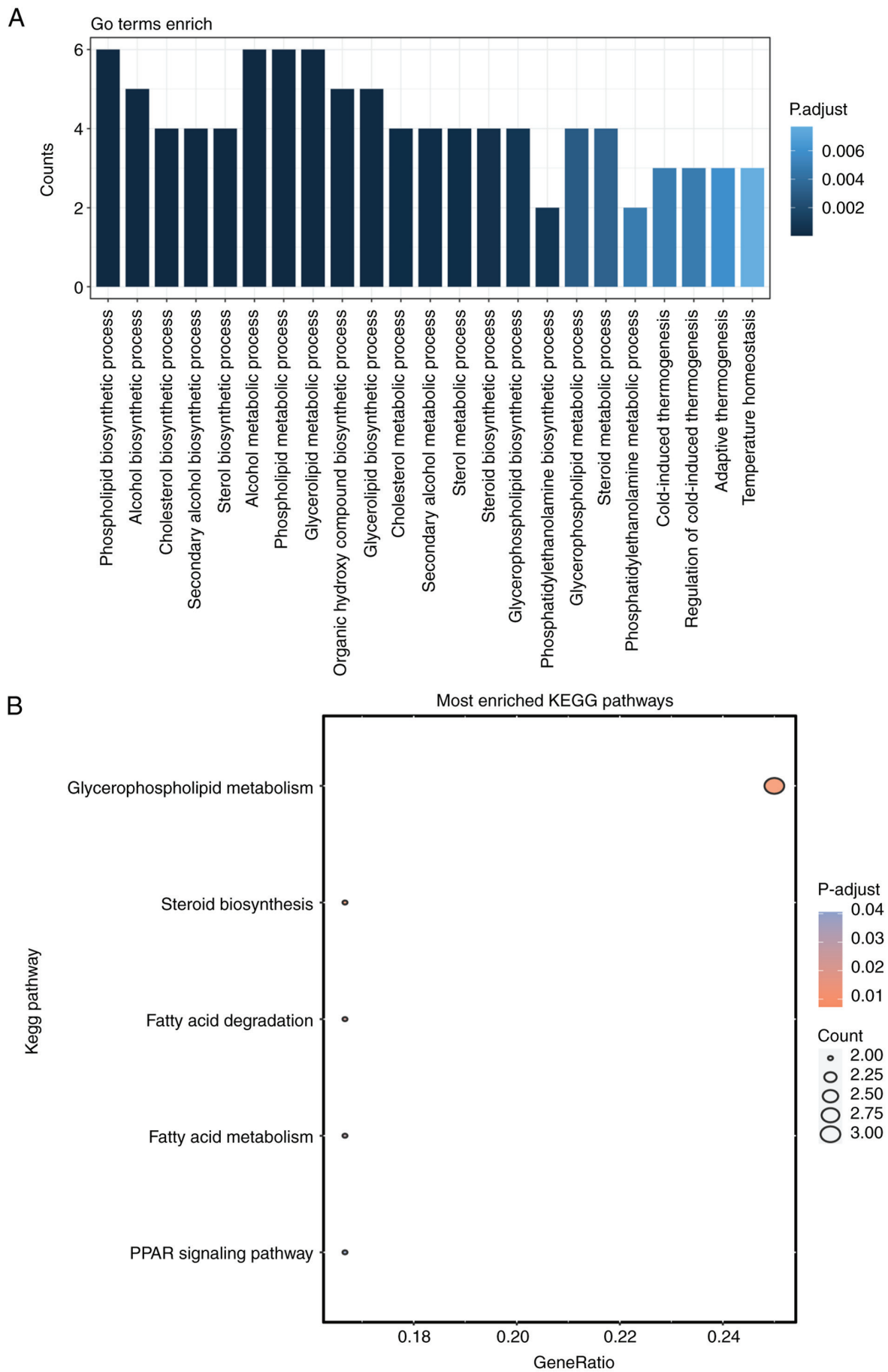


Figure 4. GO and KEGG functional enrichment analyses. (A) GO functional enrichment analysis, listing the top 10 GO entries. (B) Most enriched KEGG pathways. The x-axis shows the ratio number of genes and the y-axis shows the KEGG pathway terms. GO, Gene Ontology; KEGG, Kyoto Encyclopedia of Genes and Genomes.

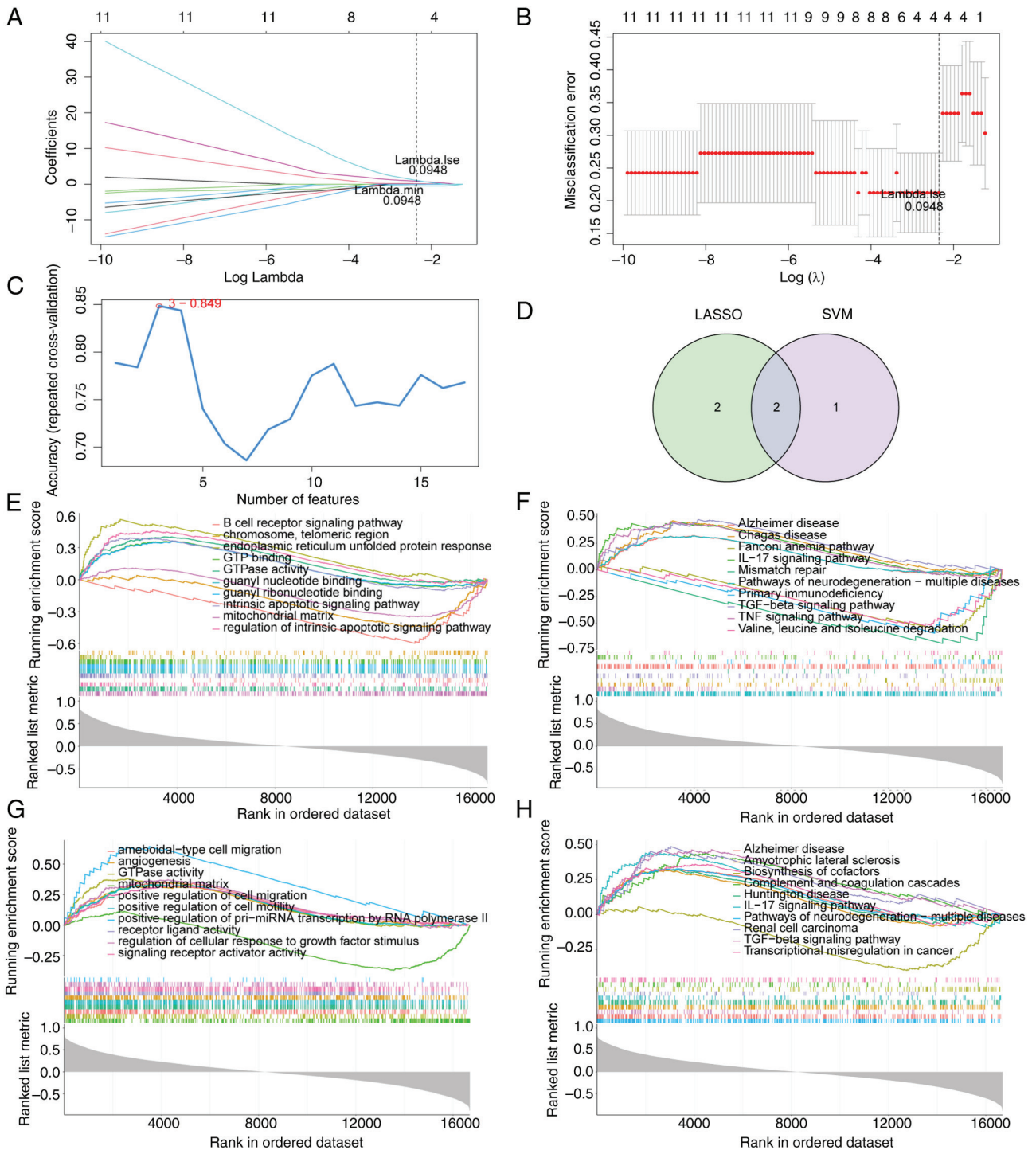


Figure 5. Identification of hub genes. (A) LASSO logistic coefficient penalty plot. Each curve represents the change of the coefficient of each independent variable. (B) Misclassification error plot. The x-axis is  $\log \lambda$  and the y-axis is the cross-validation error. The lowest error rate was achieved when  $\lambda_{\text{min}}=0.0948$ , four genes were identified as signature genes. (C) SVM-RFE algorithm, obtaining three signature genes. The y-axis shows the accuracy under different features. After selecting the first three features, the model achieved the highest accuracy. (D) Venn diagram of two overlapping genes (SAMD8 and CYP51A1) obtained through the intersections of LASSO and SVM models. (E) GSEA, the top 10 most important GO terms in SAMD8. (F) GSEA, the top 10 most important KEGG pathways of SAMD8. (G) GSEA, the top 10 most important GO terms in CYP51A1. (H) GSEA, the top 10 most important KEGG pathways of CYP51A1. LASSO, Least Absolute Shrinkage and Selector Operation; SVM, support vector machines; RFE, recursive feature elimination; GSEA, Gene Set Enrichment Analysis; GO, gene ontology; KEGG, Kyoto Encyclopedia of Genes and Genomes.

of patients with type 2 diabetes, contribute to the development and progression of lipotoxicity (55,56). Dyslipidemia and insulin resistance can disturb the function of adipose tissue, causing an increase in the plasma concentrations of NEFA, and an imbalance between pro- and anti-inflammatory

adipokines (57). This process activates intracellular lipid metabolism-related pathways, thereby promoting the deposition of fatty acids in non-adipose tissues (58). The resulting micro-inflammatory state and production of reactive oxygen species can induce lipids to undergo oxidative stress



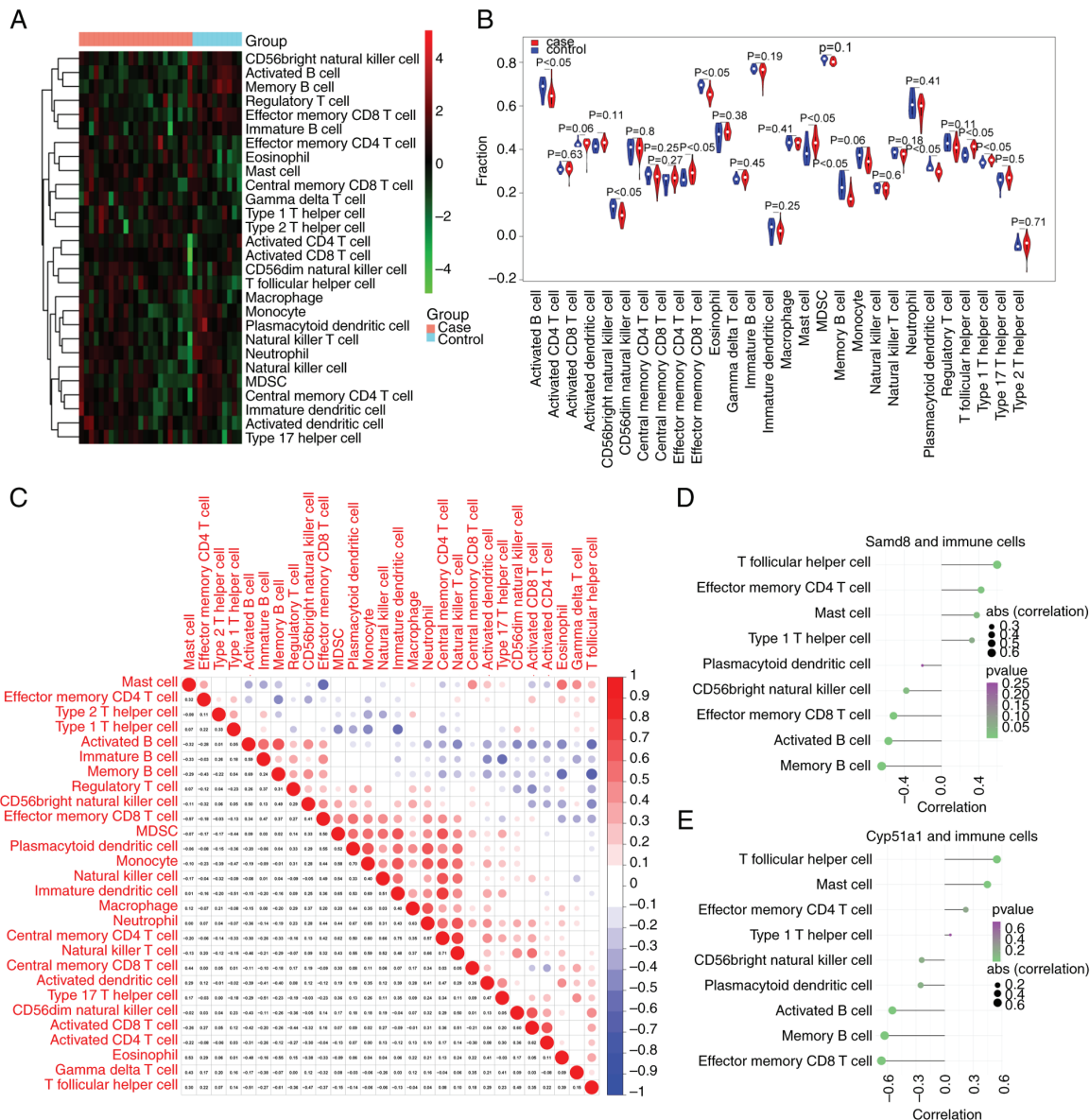


Figure 6. Analysis of immune cell infiltration landscape. (A) Heatmap of the infiltration of 28 immune cells into the DN and healthy samples. (B) Violin chart of immune cell infiltration score. There were nine immune cell types were significantly different in DN and healthy samples ( $P<0.05$ ). (C) Pearson correlation coefficients among all immune cells. Red indicates positive correlation; blue indicates negative correlation. (D) Pearson correlation coefficients among immune cells and the hub gene SAMD8. (E) Pearson correlation coefficients among immune cells and the hub gene CYP51A1. Both SAMD8 and CYP51A1 were correlated with activated B cell, effector memory CD8 T cell, memory B cell and T follicular helper cell ( $|cor|>0.5$ ,  $P<0.05$ ). DN, diabetic nephropathy.

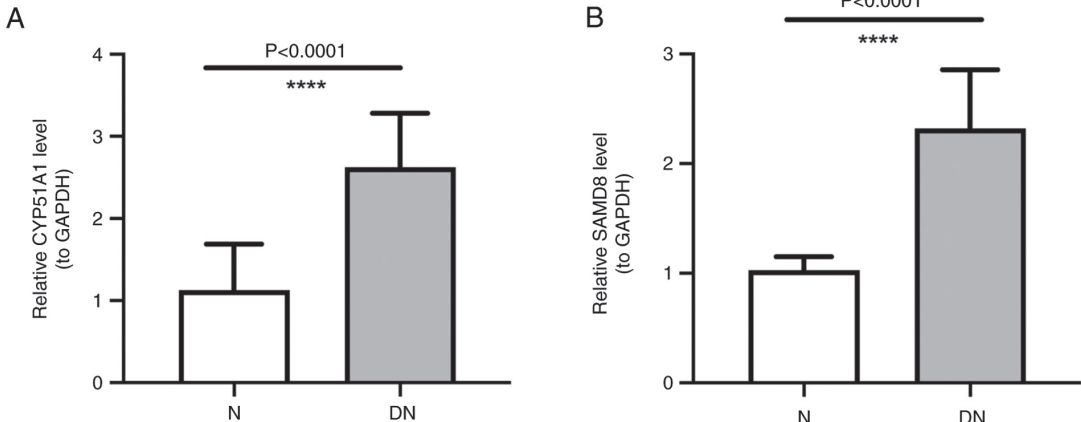


Figure 7. Reverse transcription-quantitative PCR validation. (A) Higher expression of CYP51A1 in DN blood samples. (B) Higher expression of SAMD8 in DN blood samples. \*\*\*\* $P<0.0001$ . DN, diabetic nephropathy; N, normal.

modification. The modified lipids participate in intercellular signal transduction and exacerbate inflammation, oxidative stress and lipid peroxidation (14). This cascade of events can cause cells to employ adaptive protective mechanisms of mitophagy, autophagy and apoptosis, thereby damaging the cells (18,59).

In contrast to healthy subjects, various immune cell types (activated B cells, CD56bright natural killer cells, effector memory CD4 T cells, effector memory CD8 T, mast cells, memory B cells, plasmacytoid dendritic cells, T follicular helper cells and type 1 T helper cells) exhibited different levels in patients with DN, as shown by the immune infiltration analysis. Previous studies have demonstrated that patients with DN often present with renal inflammation, which is closely associated with the onset and progression of DN (60-63). Wilson *et al* (64) reported immune cell infiltration and abnormal angiogenesis as early indicators of DN. Elevated monocyte counts and monocyte:HDL ratio can be detected in patients with DN, suggesting that monocytes play a key role in the inflammatory response to DN (65-67). According to the conventional pathological mechanisms of DN, in addition to altered hemodynamics, factors such as advanced glycation end products (AGE), oxidized lipids, free radicals and fatty acids produced from numerous biological mechanisms of glucotoxicity and lipotoxicity can cause inflammatory responses (68,69). The presence of AGE receptors in macrophages, endothelial cells and mesenchymal cells allows monocyte activation and the subsequent release of inflammatory cytokines (IL-1, IL-6, IL-18, CRP and TNF- $\alpha$ ) (66). Monocyte activation can lead to chronic inflammation and atherosclerosis in the kidney (70). Long term, these alterations can change renal hemodynamics, glomerular filtration rate and blood pressure (71). Notably, the key genes identified in the present study, SAMD8 and CYP51A1, were correlated with various immune cell types, such as activated B cells, effector memory CD8 T cells, memory B cells and T follicular helper cells. Hence, it may be suggested that these two genes could influence the development of DN not only through lipid metabolism but also by mediating the related immune processes.

There were certain limitations in the present study. Firstly, despite attempts to select a dataset with the largest possible sample size for analysis, the small sample size remained a drawback. Subsequently, the expression of SAMD8 and CYP51A1 was validated using RT-qPCR; however, protein-level validation was not performed and further investigation into the underlying mechanism was also lacking. However, the present study has some significance. It identified the key genes related to lipid metabolism in DN for the first time, and explored the signaling pathways enriched by these key genes and their relationship with the immune environment through enrichment analysis and immune infiltration analysis. The present study offers valuable insights for elucidating the relationship between DN and lipid metabolism, and for providing a new reference point for clinical treatment and diagnosis of DN. Next, the mechanism of key genes in DN will be further verified through animal modeling.

In conclusion, the present study demonstrated that SAMD8 and CYP51A1 were key hub genes responsible for lipid metabolism in DN. They were markedly upregulated in DN and closely related to the immune response in DN.

## Acknowledgements

Not applicable.

## Funding

The present study was supported by the Kunming Medical University Basic Research Joint Project (grant no. 202301AY070001-295).

## Availability of data and materials

The data analyzed in the present study may be found in the GEO database under accession number GSE142153 or at the following URL: <https://www.ncbi.nlm.nih.gov/geo/query/acc.cgi>. The other data generated in the present study may be requested from the corresponding author.

## Authors' contributions

MY wrote the manuscript and made substantial contributions to conception and design. JW and HM were responsible for data analysis and processing. JX and YX interpreted data. WK collected clinical samples and performed qPCR experiments. MY and JW confirm the authenticity of all the raw data. All authors read and approved the final version of the manuscript.

## Ethics approval and consent to participate

The present study was approved by the Ethics Committee of The First People's Hospital of Yunnan Province (approval no. 2022GJ227). Written informed consent was obtained from all participants.

## Patient consent for publication

Not applicable.

## Competing interests

The authors declare that they have no competing interests.

## References

1. Thipsawat S: Early detection of diabetic nephropathy in patient with type 2 diabetes mellitus: A review of the literature. *Diab Vasc Dis Res* 18: 14791641211058856, 2021.
2. Saran R, Robinson B, Abbott KC, Bragg-Gresham J, Chen X, Gipson D, Gu H, Hirth RA, Hutton D, Jin Y, *et al*: US renal data system 2019 annual data report: Epidemiology of kidney disease in the United States. *Am J Kidney Dis* 75 (1 Suppl 1): A6-A7, 2020.
3. Zhou Y, Echouffo-Tcheugui JB, Gu JJ, Ruan XN, Zhao GM, Xu WH, Yang LM, Zhang H, Qiu H, Narayan KM and Sun Q: Prevalence of chronic kidney disease across levels of glycemia among adults in Pudong New Area, Shanghai, China. *BMC Nephrology* 14: 253, 2013.
4. Kawanami D, Matoba K and Utsunomiya K: Signaling pathways in diabetic nephropathy. *Histol Histopathol* 31: 1059-1067, 2016.
5. Quan KY, Yap CG, Jahan NK and Pillai N: Review of early circulating biomolecules associated with diabetes nephropathy-Ideal candidates for early biomarker array test for DN. *Diabetes Res Clin Pract* 182: 109122, 2021.
6. Samsu N: Diabetic Nephropathy: Challenges in Pathogenesis, Diagnosis, and Treatment. *Biomed Res Int* 2021: 1497449, 2021.

7. Magee C, Grieve DJ, Watson CJ and Brazil DP: Diabetic nephropathy: A tangled web to unweave. *Cardiovasc Drugs* 31: 579-592, 2017.
8. Vaziri ND: Disorders of lipid metabolism in nephrotic syndrome: Mechanisms and consequences. *Kidney Int* 90: 41-52, 2016.
9. Cooper ME: Interaction of metabolic and haemodynamic factors in mediating experimental diabetic nephropathy. *Diabetologia* 44: 1957-1972, 2001.
10. Forbes JM, Fukami K and Cooper ME: Diabetic nephropathy: Where hemodynamics meets metabolism. *Exp Clin Endocrinol Diabetes* 115: 69-84, 2007.
11. Herman-Edelstein M, Scherzer P, Tobar A, Levi M and Gafter U: Altered renal lipid metabolism and renal lipid accumulation in human diabetic nephropathy. *J Lipid Res* 55: 561-572, 2014.
12. Yang W, Luo Y, Yang S, Zeng M, Zhang S, Liu J, Han Y, Liu Y, Zhu X, Wu H, *et al*: Ectopic lipid accumulation: Potential role in tubular injury and inflammation in diabetic kidney disease. *Clin Sci (Lond)* 132: 2407-2422, 2018.
13. Vallon V and Thomson SC: The tubular hypothesis of nephron filtration and diabetic kidney disease. *Nat Rev Nephrol* 16: 317-336, 2020.
14. Baum P, Toyka KV, Blüher M, Kosacka J and Nowicki M: Inflammatory mechanisms in the pathophysiology of diabetic peripheral neuropathy (DN)-New aspects. *Int J Mol Sci* 22: 10835, 2021.
15. Kawanami D, Matoba K and Utsunomiya K: Dyslipidemia in diabetic nephropathy. *Ren Replace Ther* 2: 16, 2016.
16. Lu CC, Ma KL, Ruan XZ and Liu BC: The emerging roles of microparticles in diabetic nephropathy. *Int J Biol Sci* 13: 1118-1125, 2017.
17. Ferrara D, Montecucco F, Dallegrì F and Carbone F: Impact of different ectopic fat depots on cardiovascular and metabolic diseases. *J Cell Physiol* 234: 21630-21641, 2019.
18. Nishi H, Higashihara T and Inagi R: Lipotoxicity in kidney, heart, and skeletal muscle dysfunction. *Nutrients* 11: 1664, 2019.
19. Xu T, Xu X, Zhang L, Zhang K, Wei Q, Zhu L, Yu Y, Xiao L, Lin L, Qian W, *et al*: Lipidomics reveals serum specific lipid alterations in diabetic nephropathy. *Front Endocrinol (Lausanne)* 12: 781417, 2021.
20. Wu L, Liu C, Chang DY, Zhan R, Zhao M, Man Lam S, Shui G, Zhao MH, Zheng L and Chen M: The attenuation of diabetic nephropathy by annexin A1 via regulation of lipid metabolism through the AMPK/PPAR $\alpha$ /CPT1b pathway. *Diabetes* 70: 2192-2203, 2021.
21. Thongnak L, Pongchaidecha A and Lungkaphin A: Renal lipid metabolism and lipotoxicity in diabetes. *Am J Med Sci* 359: 84-99, 2020.
22. Zhao YH and Fan YJ: Resveratrol improves lipid metabolism in diabetic nephropathy rats. *Front Biosci (Landmark Ed)* 25: 1913-1924, 2020.
23. Han Y, Xiong S, Zhao H, Yang S, Yang M, Zhu X, Jiang N, Xiong X, Gao P, Wei L, *et al*: Lipophagy deficiency exacerbates ectopic lipid accumulation and tubular cells injury in diabetic nephropathy. *Cell Death Dis* 12: 1031, 2021.
24. Patel D and Witt SN: Ethanolamine and Phosphatidylethanolamine: Partners in health and disease. *Oxid Med Cell Longev* 2017: 4829180, 2017.
25. van der Veen JN, Kennelly JP, Wan S, Vance JE, Vance DE and Jacobs RL: The critical role of phosphatidylcholine and phosphatidylethanolamine metabolism in health and disease. *Biochim Biophys Acta Biomembr* 1859 (9 Pt B): 1558-1572, 2017.
26. Ravandi A, Kuksis A and Shaikh NA: Glucosylated Glycerophosphoethanolamines are the Major LDL glycation products and increase LDL susceptibility to oxidation evidence of their presence in atherosclerotic lesions. *Arterioscler Thromb Vasc Biol* 20: 467-477, 2000.
27. Vlassara H and Palace MR: Glycoxidation: The menace of diabetes and aging. *Mt Sinai J Med* 70: 232-241, 2003.
28. Sur S, Nguyen M, Boada P, Sigdel TK, Sollinger H and Sarwal MM: FcER1: A novel molecule implicated in the progression of human diabetic kidney disease. *Front Immunol* 12: 769972, 2021.
29. Ritchie ME, Phipson B, Wu D, Hu Y, Law CW, Shi W and Smyth GK: limma powers differential expression analyses for RNA-sequencing and microarray studies. *Nucleic Acids Res* 43: e47, 2015.
30. Ito K and Murphy D: Application of ggplot2 to Pharmacometric Graphics. *CPT Pharmacometrics Syst Pharmacol* 2: e79, 2013.
31. Hu K: Become competent in generating RNA-Seq heat maps in one day for novices without prior R experience. *Methods Mol Biol* 2239: 269-303, 2021.
32. Chen H and Boutros PC: VennDiagram: A package for the generation of highly-customizable Venn and Euler diagrams in R. *BMC Bioinformatics* 12: 35, 2011.
33. Tang J, Kong D, Cui Q, Wang K, Zhang D, Gong Y and Wu G: Prognostic genes of breast cancer identified by gene co-expression network analysis. *Front Oncol* 8: 374, 2018.
34. Langfelder P and Horvath S: WGCNA: An R package for weighted correlation network analysis. *BMC Bioinformatics* 9: 559, 2008.
35. Szklarczyk D, Gable AL, Nastou KC, Lyon D, Kirsch R, Pyysalo S, Doncheva NT, Legeay M, Fang T, Bork P, *et al*: The STRING database in 2021: Customizable protein-protein networks, and functional characterization of user-uploaded gene/measurement sets. *Nucleic Acids Res* 49 (D1): D605-D612, 2021.
36. Wu T, Hu E, Xu S, Chen M, Guo P, Dai Z, Feng T, Zhou L, Tang W, Zhan L, *et al*: clusterProfiler 4.0: A universal enrichment tool for interpreting omics data. *Innovation (Camb)* 2: 100141, 2021.
37. Walter W, Sanchez-Cabo F and Ricote M: GOplot: An R package for visually combining expression data with functional analysis. *Bioinformatics* 31: 2912-2914, 2015.
38. Xu Q, Xu H, Deng R, Wang Z, Li N, Qi Z, Zhao J and Huang W: Multi-omics analysis reveals prognostic value of tumor mutation burden in hepatocellular carcinoma. *Cancer Cell Int* 21: 342, 2021.
39. Zhang M, Zhu K, Pu H, Wang Z, Zhao H, Zhang J and Wang Y: An immune-related signature predicts survival in patients with lung adenocarcinoma. *Front Oncol* 9: 1314, 2019.
40. Sanz H, Valim C, Vegas E, Oller JM and Reverter F: SVM-RFE: Selection and visualization of the most relevant features through non-linear kernels. *BMC Bioinformatics* 19: 432, 2018.
41. Hänzelmann S, Castelo R and Guinney J: GSVA: Gene set variation analysis for microarray and RNA-seq data. *BMC Bioinformatics* 14: 7, 2013.
42. Pei L, Li J, Xu Z, Chen N, Wu X and Chen J: Effect of high hydrostatic pressure on aroma components, amino acids, and fatty acids of Hami melon (*Cucumis melo* L. var. *reticulatus* naud.) juice. *Food Sci Nutr* 8: 1394-1405, 2020.
43. Strezoska Ž, Licon A, Haimes J, Spayd KJ, Patel KM, Sullivan K, Jastrzebski K, Simpson KJ, Leake D, van Brabant Smith A and Vermeulen A: Optimized PCR conditions and increased shRNA fold representation improve reproducibility of pooled shRNA screens. *PLoS One* 7: e42341, 2012.
44. Cabukusta B, Nettebrock NT, Kol M, Hilderink A, Tafesse FG and Holthuis JCM: Ceramide phosphoethanolamine synthase SMSr is a target of caspase-6 during apoptotic cell death. *Biosci Rep* 37: BSR20170867, 2017.
45. Tafesse FG, Vacaru AM, Bosma EF, Hermansson M, Jain A, Hilderink A, Somerharju P and Holthuis JC: Sphingomyelin synthase-related protein SMSr is a suppressor of ceramide-induced mitochondrial apoptosis. *J Cell Sci* 127 (Pt 2): 445-454, 2014.
46. Srivastava SP, Shi S, Koya D and Kanasaki K: Lipid mediators in diabetic nephropathy. *Fibrogenesis Tissue Repair* 7: 12, 2014.
47. Woodcock J: Sphingosine and ceramide signalling in apoptosis. *IUBMB Life* 58: 462-466, 2006.
48. Tani M, Ito M and Igarashi Y: Ceramide/sphingosine/sphingosine 1-phosphate metabolism on the cell surface and in the extracellular space. *Cell Signal* 19: 229-237, 2007.
49. Kuzmenko DI and Klimentyeva TK: Role of ceramide in apoptosis and development of insulin resistance. *Biochemistry (Mosc)* 81: 913-927, 2016.
50. Summers SA: The ART of lowering ceramides. *Cell Metab* 22: 195-196, 2015.
51. Symons JD and Abel ED: Lipotoxicity contributes to endothelial dysfunction: A focus on the contribution from ceramide. *Rev Endocr Metab Disord* 14: 59-68, 2013.
52. Chavez JA and Summers SA: A ceramide-centric view of insulin resistance. *Cell Metab* 15: 585-594, 2012.
53. Park JW, Byrd A, Lee CM and Morgan ET: Nitric oxide stimulates cellular degradation of human CYP51A1, the highly conserved lanosterol 14 $\alpha$ -demethylase. *Biochem J* 474: 3241-3252, 2017.
54. Kaluzhskiy L, Ershov P, Yablokov E, Shkel T, Grabovec I, Mezentsev Y, Gnedenko O, Usanov S, Shabunya P, Fatykhava S, *et al*: Human Lanosterol 14-Alpha Demethylase (CYP51A1) is a putative target for natural flavonoid luteolin 7,3'-Disulfate. *Molecules* 26: 2237, 2021.
55. Opazo-Ríos L, Mas S, Marín-Royo G, Mezzano S, Gómez-Guerrero C, Moreno JA and Egido J: Lipotoxicity and diabetic nephropathy: Novel mechanistic insights and therapeutic opportunities. *Int J Mol Sci* 21: 2632, 2020.

56. Charles MA, Eschwège E, Thibault N, Claude JR, Warnet JM, Rosselin GE, Girard J and Balkau B: The role of non-esterified fatty acids in the deterioration of glucose tolerance in Caucasian subjects: Results of the Paris Prospective Study. *Diabetologia* 40: 1101-1106, 1997.
57. Meex RCR, Blaak EE and van Loon LJC: Lipotoxicity plays a key role in the development of both insulin resistance and muscle atrophy in patients with type 2 diabetes. *Obes Rev* 20: 1205-1217, 2019.
58. Gai Z, Wang T, Visentin M, Kullak-Ublick GA, Fu X and Wang Z: Lipid accumulation and chronic kidney disease. *Nutrients* 11: 722, 2019.
59. Jaishy B and Abel ED: Lipids, lysosomes, and autophagy. *J Lipid Res* 57: 1619-1635, 2016.
60. Pérez-Morales RE, Del Pino MD, Valdivielso JM, Ortiz A, Mora-Fernández C and Navarro-González JF: Inflammation in diabetic kidney disease. *Nephron* 143: 12-16, 2019.
61. Shao BY, Zhang SF, Li HD, Meng XM and Chen HY: Epigenetics and inflammation in diabetic nephropathy. *Front Physiol* 12: 649587, 2021.
62. Wang Y, Zhao M and Zhang Y: Identification of fibronectin 1 (FN1) and complement component 3 (C3) as immune infiltration-related biomarkers for diabetic nephropathy using integrated bioinformatic analysis. *Bioengineered* 12: 5386-5401, 2021.
63. Huang M, Zhu Z, Nong C, Liang Z, Ma J and Li G: Bioinformatics analysis identifies diagnostic biomarkers and their correlation with immune infiltration in diabetic nephropathy. *Ann Transl Med* 10: 669, 2022.
64. Wilson PC, Wu H, Kirita Y, Uchimura K, Ledru N, Rennke HG, Welling PA, Waikar SS and Humphreys BD: The single-cell transcriptomic landscape of early human diabetic nephropathy. *Proc Natl Acad Sci USA* 116: 19619-19625, 2019.
65. Onalan E: The relationship between monocyte to high-density lipoprotein cholesterol ratio and diabetic nephropathy. *Pak J Med Sci* 35: 1081-1086, 2019.
66. Huang Q, Wu H, Wo M, Ma J, Fei X and Song Y: Monocyte-lymphocyte ratio is a valuable predictor for diabetic nephropathy in patients with type 2 diabetes. *Medicine (Baltimore)* 99: e20190, 2020.
67. Efe FK: The association between monocyte HDL ratio and albuminuria in diabetic nephropathy. *Pak J Med Sci* 37: 1128-1132, 2021.
68. Ancuta P, Wang J and Gabuzda D: CD16+ monocytes produce IL-6, CCL2, and matrix metalloproteinase-9 upon interaction with CX3CL1-expressing endothelial cells. *J Leukoc Biol* 80: 1156-1164, 2006.
69. Tang G, Li S, Zhang C, Chen H, Wang N and Feng Y: Clinical efficacies, underlying mechanisms and molecular targets of Chinese medicines for diabetic nephropathy treatment and management. *Acta Pharm Sin B* 11: 2749-2767, 2021.
70. Ji L, Chen Y, Wang H, Zhang W, He L, Wu J and Liu Y: Overexpression of Sirt6 promotes M2 macrophage transformation, alleviating renal injury in diabetic nephropathy. *Int J Oncol* 55: 103-115, 2019.
71. Wolf G: New insights into the pathophysiology of diabetic nephropathy: From haemodynamics to molecular pathology. *Eur J Clin Invest* 34: 785-796, 2004.



Copyright © 2024 Yang et al. This work is licensed under a Creative Commons Attribution-NonCommercial-NoDerivatives 4.0 International (CC BY-NC-ND 4.0) License.